Study on dynamic response of high speed train window glass under tunnel aerodynamic effects

Received 29 March 2023
Revised 10 April 2023
Accepted 10 April 2023

Xiaogen Liu and Shuang Qi
The State Key Laboratory of Green Building Materials, China Building Materials Academy, Beijing, China, and
Detian Wan and Dezhi Zheng
China Testing & Certification International Group Co., Ltd, China Building Materials Academy, Beijing, China

Abstract

Purpose – This paper aims to analyze the bearing characteristics of the high speed train window glass under aerodynamic load effects.

Design/methodology/approach – In order to obtain the dynamic strain response of passenger compartment window glass during high-speed train crossing the tunnel, taking the passenger compartment window glass of the CRH3 high speed train on Wuhan–Guangzhou High Speed Railway as the research object, this study tests the strain dynamic response and maximum principal stress of the high speed train passing through the tunnel entrance and exit, the tunnel and tunnel groups as well as trains meeting in the tunnel at an average speed of 300 km·h-1.

Findings – The results show that while crossing the tunnel, the passenger compartment window glass of high speed train is subjected to the alternating action of positive and negative air pressures, which shows the typical mechanic characteristics of the alternating fatigue stress of positive-negative transient strain. The maximum principal stress of passenger compartment window glass for high speed train caused by tunnel aerodynamic effects does not exceed 5 MPa, and the maximum value occurs at the corresponding time of crossing the tunnel groups. The high speed train window glass bears medium and low strain rates under the action of tunnel aerodynamic effects, while the maximum strain rate occurs at the meeting moment when the window glass meets the train head approaching from the opposite side in the tunnel. The shear modulus of laminated glass PVB film that makes up high speed train window glass is sensitive to the temperature and action time. The dynamically equivalent thickness and stiffness of the laminated glass and the dynamic bearing capacity of the window glass decrease with the increase of the action time under tunnel aerodynamic pressure. Thus, the influence of the loading action time and fatigue under tunnel aerodynamic effects on the glass strength should be considered in the design for the bearing performance of high speed train window glass.

Originality/value – The research results provide data support for the analysis of mechanical characteristics, damage mechanism, strength design and structural optimization of high speed train glass.

Keywords High speed train window glass, Tunnel aerodynamic effect, Strain dynamic response, Maximum principal stress, Strain rate, Bearing characteristics

Paper type Research paper

1. Introduction

High speed railway lines in challenging mountainous areas generally pass through mountains or hills in the form of long and large tunnels and tunnel groups to ensure a smooth

Funding: The research was supported by the National Natural Science Foundation of China (Grant Nos. 52072356 and 52032011) and the 2019 Zaozhuang High-level Talents Project (Grant No. ZZYF-01).

traffic. The high speed railway traffic environment in challenging mountainous areas in China features numerous tunnels, large proportion of long and extra-long tunnels and widely distributed tunnel groups. With the continuous improvement of the running speed of high speed trains, the dynamic effect between trains and surrounding air is obviously intensified; in particular, the tunnel aerodynamic effect induced by trains running at high speed in tunnels has a great impact on the running environment and safety of trains (Tian, 2015).The tunnel aerodynamic effect is particularly adverse to the high speed train window glass, the weakest part of the whole train. The glass damage rate of high speed trains passing through tunnels is much higher than that of high speed trains running on plain areas.

Previous studies have shown that the aerodynamic pressure generated when a high speed train passes through a tunnel is proportional to the square of the running speed (Wang, Luo, Gao, Li, & Li, 2020). Since the 1960s, Ozawa (1979) proposed an empirical formula for calculating the amplitude and waveform of the compression wave at the tunnel entrance according to the results of the online full-scale train test on Shinkansen in Japan to identify the formation mechanism and influencing factors of aerodynamic pressure change induced by train entering the tunnel; Woods and Pope (1979) proposed an empirical formula for calculating the compression wave at the tunnel entrance based on the results of the full-scale train test of the Patchway single-track tunnel on the London–South Wales railway line, as well as a quasi-static one-dimensional flow model describing the flow field when the train passes through the tunnel. With the continuous development of modern computer and numerical simulation technology, researchers have applied two-dimensional and three-dimensional numerical simulation for the analysis on tunnel aerodynamic effects (Iyer, Kim, & Kim, 2018; Real, Zamorano, Ribes, & Real, 2015), and proposed a series of field measurement methods and devices (Doi, Ogawa, Masubuchi, & Kaku, 2010; Ko, Chen, Hoe, & Wang, 2012), effectively improving the calculation and measurement accuracy of pressure waves of tunnel aerodynamic effects. Since the 1990s, China Academy of Railway Sciences and other institutes successively carried out on-site full-scale train tests on Suining–Chongqing Railway (Academy of Railway Sciences Chengdu Railway Bureau, Ministry of Railways, 2005), Wuhan–Guangzhou High Speed Railway (Academy of Railway Sciences, 2009), Zhengzhou–Xi'an High Speed Railway (Chen, Zhang, He, & Huang, 2014), etc. and systematically studied the tunnel aerodynamic effects caused by trains running at a speed of 200-250 $km \cdot h^{-1}$ and 300-350 $km \cdot h^{-1}$, respectively, and investigated their laws, providing important theoretical, experimental and calculation data support for the development of high speed railways in China and the speed-up of railways in western mountainous areas. Shi (2002) and Jing, Liu, and Ren (2019) analyzed the train and window structure based on ANSYS/DYNA analysis software, and obtained the curve of window glass stress changing with time under the action of pressure waves generated at high speed trains meeting and the typical transient response (stress and lateral displacement) of the car body and side windows, respectively. Tian, Yao, and Yao (2000) analyzed the car body steel structure and windows of the train under the action of impact load of transient pressure, and assessed the ability of existing trains on the existing lines to withstand the pressure waves generated at high speed trains meeting. Qian, Zheng, Yu, and Li (2013) simulated the dynamic response process of high speed train carriages under the action of pressure waves generated when trains met on the open track at three constant speeds (250, 350 and 500 $km \cdot h^{-1}$), and obtained the change curve of Mises stress in the center of the side window with time. Wang (2020) studied the dynamic stress response characteristics of the side window glass of the cab when the train was passing through the Qinling Tunnel and its optimization scheme.

The aerodynamic load change caused by the train passing through the tunnel is extremely complex, and the magnitude and direction of air pressure acting on the glass surface show a fatigue transient dynamic process, which is obviously different from the bearing and damage mechanism of glass under conventional static load (Deng *et al.*, 2021; Nie, Chen, Sun, & Templeton, 2007; Peng, Ma, Wang, Wang, & Gao, 2019). So far, no sufficient consideration is given to the adverse impact of the aerodynamic effects on the high speed train window glass generated when the train passes through the tunnel; therefore, it is hard to identify the mechanical characteristics, failure mechanism, strength threshold and damage prevention mechanism of the high speed train window glass resulting from the tunnel aerodynamic load.

In this paper, the strain dynamic response of the window glass during high speed train passing through the tunnel is measured based on the characteristic that the resistance strain and the tunnel aerodynamic load acting on the train window glass change in a coordinated manner. The acting mode and characteristics of the tunnel aerodynamic effect on the train window glass can be accurately identified by analyzing the strain response curve and the bearing performance of the train window glass under the action of aerodynamic load, so as to provide data support for the analysis of stress characteristics, damage mechanism, strength design and structure optimization of the high speed train window glass.

2. Measurement of strain dynamic response

2.1 Test object

The passenger compartment window glass of two groups of 16-car CRH3 trains on Wuhan–Guangzhou High Speed Railway is selected for testing. The glass specification, structure and installation diagram are shown in Figure 1. In the figure, the black part of the laminated glass is a 1.52 mm-thick PVB film.

The size of the glass is 1,480 mm × 800 mm (L x W), and the distance between the glass under test (located in the fifth car) and the train nose is about 120 m. The tunnels through which the trains pass are double-track tunnels and mainly concentrated in the border area between Hunan Province and Guangdong Province.

2.2 Test equipment and parameters

The eight-channel INV3062C1(S) dynamic strain acquisition device is used, and the test acquisition frequency is 20 kHz. For the resistance strain gauge, strain rosette (model: BE120-1CA-Q30 P400) is used, with a resistance value of 120 Ω and a sensitivity coefficient of 2.10%.

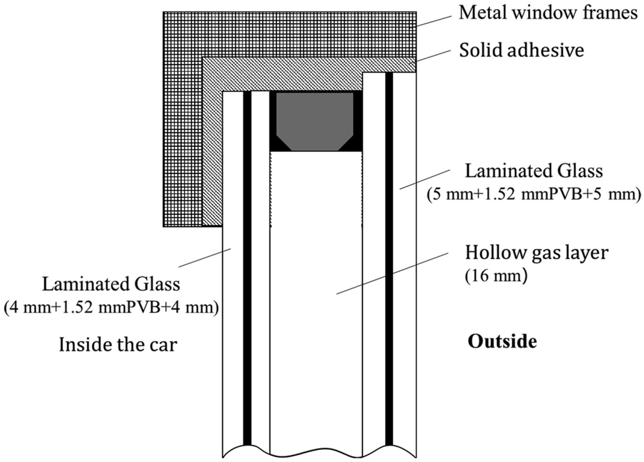

Source(s): Authors own work

Figure 1. Specification, structure and installation diagram of train window glass under test

2.3 Measurement process

Since the pressure increase of the car body near the tunnel wall face is significantly greater than that of the other side of the car body when the train enters the tunnel, and in addition to analyzing the impact of the air pressure on the train window glass at the time of meeting, the passenger compartment window glass near the tunnel wall face is measured. As shown in Figure 2, the strain rosette is attached firmly to the center of the glass facing the inside of the car. The strain at this position is the maximum when the glass is subjected to uniform pressure, and the strain value is negative when the glass is subjected to positive pressure outside the car, and positive when the glass is subjected to negative pressure outside the car. The strain rosette is connected with the strain acquisition device, and the strain response process of the passenger compartment window glass in the directions of 0°, 45° and 90° during the train passing through the tunnel is collected by computer. The test is conducted at an average train running speed of 300 km · h^{-1}, and the corresponding average ambient temperature at the time of testing is 25℃.

Before the test, the strain value is subject to null shift to eliminate other influencing factors. Then, the strain dynamic responses of the passenger compartment window glass are tested, respectively, when the train enters the tunnel entrance, passes through the tunnel exit, the whole tunnel and the tunnel groups and meets the other train in the tunnel.

3. Results and discussions

3.1 Strain dynamic response process of passenger compartment window glass

3.1.1 Entering the tunnel entrance. The dynamic response curve of the strain of the glass under test in the *X* direction with time when the train enters the tunnel entrance is shown in Figure 3. In the figure, the glass under test enters the tunnel at 1.5 s.

It can be seen from Figure 3 that the tunnel aerodynamic effect began to be obvious about 2 s after the glass under test entered the tunnel. This is mainly due to the fact that the aerodynamic pressure peak formed when the train entered the tunnel mainly occurred in front of the train nose, and the front-end compressed air flowed backward through the annular space between the train and the tunnel wall face, so the glass under test was temporarily not affected (Zhao, Ma, Cheng, & Zhang, 2012). The glass under test was subjected to the fluctuation process of positive strain → negative strain → positive strain →

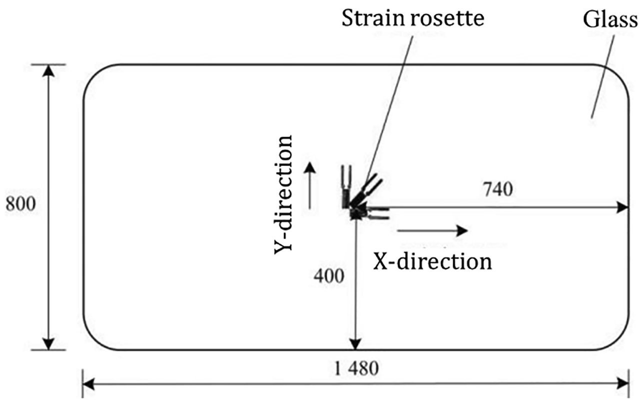

Source(s): Authors own work

Figure 2.
Schematic diagram of attaching method and position of strain rosette (Unit: mm)

returning to normal, with a total action time of about 6.5 s, and the maximum strain rate occurred at the moment when the first positive strain reached the peak.

3.1.2 Passing through the tunnel exit. The dynamic response curve of the strain of the glass under test in the X direction with time when the train passes through the tunnel exit is shown in Figure 4. In the figure, the glass under test leaves the tunnel exit at 3.0 s.

It can be seen from Figure 4 that the glass under test began to be subjected to negative strain about 1.7 s before it exited the tunnel, and then the negative strain decreased rapidly to the extreme. The negative strain began to decrease after the extreme was maintained for about 3 s (1.5 s after exiting the tunnel), and it returned to the initial state about 6 s after the train exited the tunnel. During the whole process of the train passing through the tunnel exit, since the glass under test was mainly subject to the expansion wave reflected from the exit, it was only subject to negative strain with a total action time of about 7.5 s; the maximum strain rate occurred at the corresponding time of 1.5-1.7 s before the train exited the tunnel.

3.1.3 Passing through the whole tunnel. The length of the tunnel has a certain impact on the aerodynamic effect caused by the train running. The strain dynamic response process of the passenger compartment window glass under test when the train passes through the extra-long tunnel (with a total length of more than 10 km), the medium-long tunnel (with a total length of 500-3,000 m) and the medium-short tunnel (with a total length of less than 500 m) is shown in Figure 5. In the figure, the total length of the extra-long tunnel is about 12.5 km; that of the medium-long tunnel is about 2.0 km; that of the medium-short tunnel is about 500 m.

It can be seen from Figure 5 that the train took 150 s to pass though the extra-long tunnel selected for the test. After entering the tunnel, with the sudden change of strain caused by

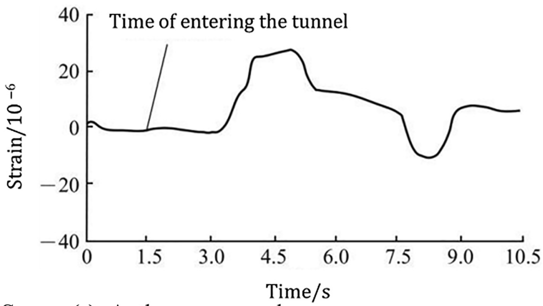

Source(s): Authors own work

Figure 3. Strain dynamic response curve of the glass under test when entering the tunnel entrance

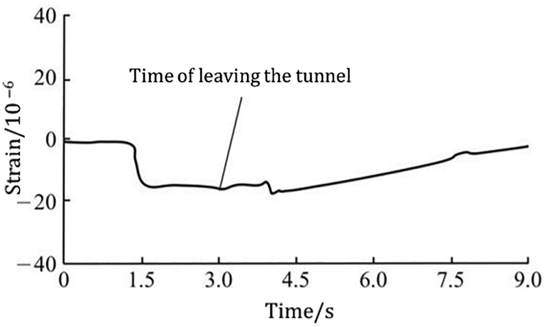

Source(s): Authors own work

Figure 4. Strain dynamic response curve of the glass under test when the train passing through the tunnel exit

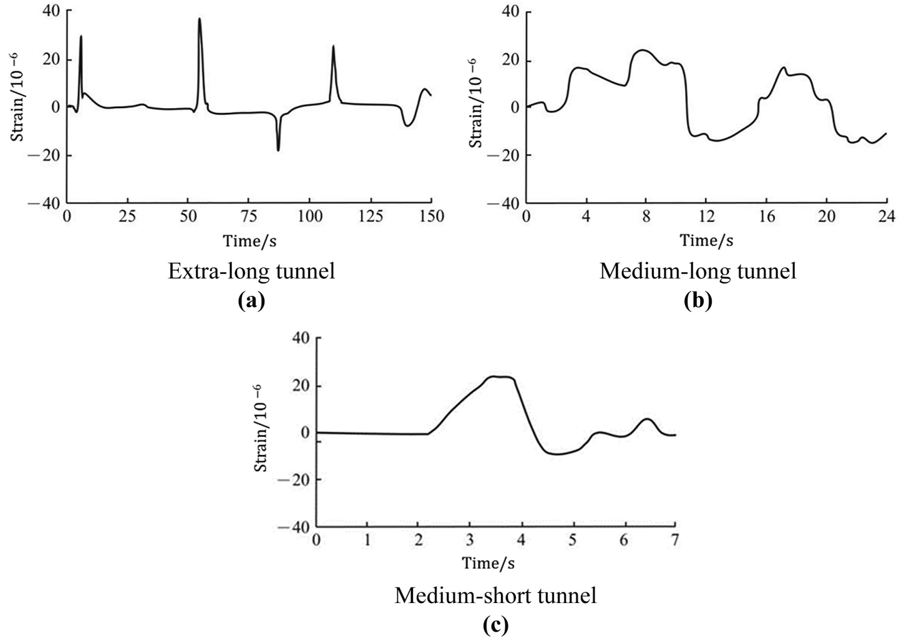

Figure 5. Strain dynamic response curve of the glass under test during the train passing through the whole tunnel

Source(s): Authors own work

entering and exiting the tunnel neglected, the glass under test had three obvious sudden change fluctuation processes of positive strain → negative strain → positive strain in the tunnel, with each sudden change of strain lasting for about 2 s; the train took 24 s to pass through the medium-long tunnel selected for the test, and the overall change rules of the strain response curve of the glass under test were basically the same as those in the case of passing through the extra-long tunnel, but the strain extreme of the glass under test in the case of the extra-long tunnel was about 20% larger than that in the case of the medium-long tunnel; the train took 6 s to pass through the medium-short tunnel selected for the test, during which the glass under test had no obvious sudden change of strain except at the time of entering the tunnel. In the process of passing through the whole tunnel, the strain fluctuation process of the high speed train window glass was consistent with that described in Zhao *et al.*'s (2012) research, that is, the tail-end expansion wave and the front-end compression wave formed by running in the tunnel were reflected and transmitted many times at both ends of the tunnel and the annular space, so that the compression wave and the expansion wave were superimposed on each other, forming a complex positive and negative fluctuation process of the air pressure field in the tunnel with time.

3.1.4 Passing through the tunnel group. Tunnel group refers to a group or groups of tunnels with the distance between adjacent tunnel portals less than the length of a passenger train. In mountainous areas, high speed railway lines generally pass through in the form of tunnel groups. The strain dynamic response curve of the window glass under test when the train passes through a tunnel group composed of four tunnels and passes through the sections between portals of adjacent tunnels for a short time is shown in Figure 6. In the figure, during passing through the tunnel groups, the train passes through the sections between portals of two adjacent tunnels for three consecutive times at 10 s, 43 s and 61 s, respectively.

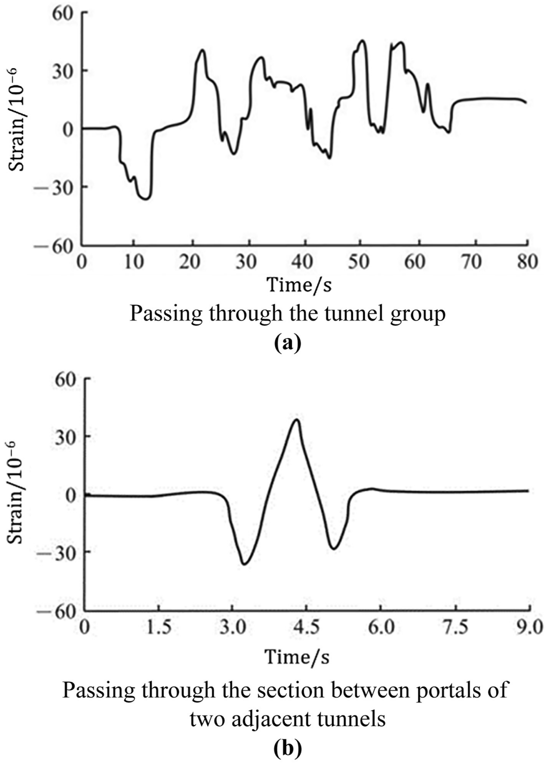

Source(s): Authors own work

Figure 6. Strain dynamic response curve of the glass under test when the train passing through the tunnel groups

It can be seen from Figure 6 that when the train passed through the section between portals of two adjacent tunnels in the tunnel group, the glass under test was disturbed by the alternating action of positive and negative air pressures; the details of the strain dynamic response when the train passed through the section between portals of two adjacent tunnels for a short time show that the glass under test quickly experienced an alternating process of negative strain → positive strain → negative strain, and the maximum strain rate occurred at the corresponding moment when the negative strain peak changed to the positive strain peak. In the process of passing through the tunnel group, the glass under test experienced rapid alternating fatigue changes of positive and negative strains, which was particularly detrimental to the service safety of train window glass.

3.1.5 Meeting in the tunnel. When two trains meet in the tunnel at an average speed of 300 $km \cdot h^{-1}$, the strain dynamic response curves of the glass under test near the meeting face and adjacent to the tunnel wall face are shown in Figure 7.

It can be seen from Figure 7 that when the glass under test near the meeting face met the nose of the opposite train, the strain suddenly changed from negative strain to positive strain, and the positive strain extreme was larger than the negative strain extreme. The positive strain continued to increase during the subsequent car body meeting, and then dropped sharply when the train met the tail of the opposite train, and then the positive strain remained stable; the maximum strain rate of the glass under test near the meeting face occurred when it

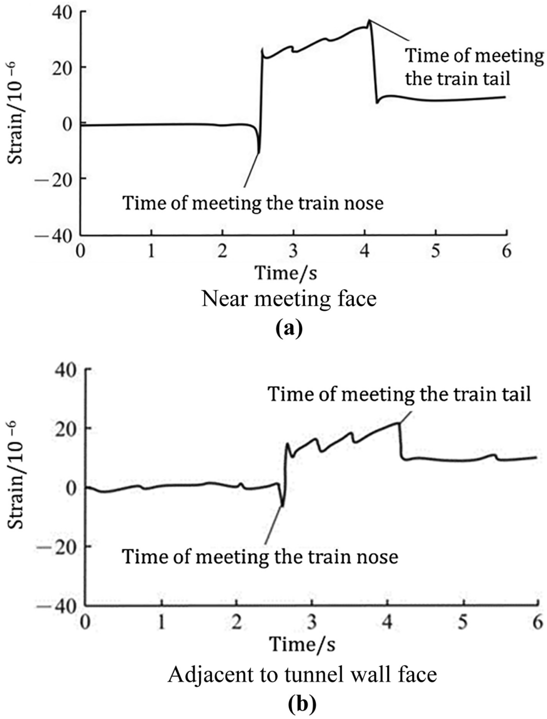

Figure 7.
Strain dynamic response curves of the glass under test during meeting in tunnel

Source(s): Authors own work

met the nose and tail of the opposite train. The strain dynamic response curve trend of the glass under test (with the same specification and size as the glass under test near the meeting face) near the tunnel wall face is basically the same as that of the glass under test near the meeting face, but the positive strain extreme in this case is about 70% of that of the glass under test near the meeting face, indicating that the glass under test near the meeting face is subject to greater aerodynamic pressure during meeting in the tunnel.

3.2 Stress extremes of passenger compartment window glass under tunnel aerodynamic effect

According to the three-dimensional strain of the glass tested by the strain rosette given in Section 2.3, the maximum principal stress σ_{max} of the passenger compartment window glass under the action of tunnel aerodynamic load can be obtained, and the calculation formula is as follows:

$$\sigma_{\max} = \frac{E}{2}\left[\frac{\varepsilon_0 + \varepsilon_{90}}{1-\mu} + \frac{1}{1+\mu}\sqrt{(\varepsilon_0 - \varepsilon_{90})^2 + (2\varepsilon_{45} - \varepsilon_0 - \varepsilon_{90})^2}\right] \quad (1)$$

where, ε_0 is the strain in the direction of 0°; ε_{45} is the strain at a 45° angle; ε_{90} is the strain at a 90° angle; E is the elastic modulus of tempered glass, taken as 72 GPa; μ is the Poisson's ratio of glass material, taken as 0.24.

See Table 1 for the results of the strain extremes of the passenger compartment window glass under test in each direction, the maximum principal stress, the maximum strain rate and the action time when the high speed train passes through different parts of the tunnel.

Table 1. Strain extremes, maximum principal stress and maximum strain rate and action time in each direction

Through the tunnel area	Direction of strain	Measured maximum strain/με 0°	45°	90°	Maximum principal stress/MPa	Total action time/s	Maximum strain rate $\mu\varepsilon/s^{-1}$	Maximum strain rate action time/s
Entering the tunnel entrance	Positive strain polarity	30.23	18.15	14.80	2.65	6.5	40.0	0.7
	Negative strain poles	−18.30	−11.34	−10.72	−1.09			
Exit through the tunnel	Positive strain polarity	0	0	0	0	7.5	90.0	0.2
	Negative strain poles	−20.10	−9.92	−4.55	−0.70			
Through extra-long tunnels (12.5 km)	Positive strain polarity	36.02	20.45	15.93	3.13		35.0	1.0
	Negative strain poles	−10.31	−5.66	−4.25	−0.49			
Through the medium-length tunnel (2.0 km)	Positive strain polarity	29.81	18.30	16.43	2.67		32.0	1.0
	Negative strain poles	−18.01	−4.25	−3.03	−0.43			
Crossing the short tunnel (0.5 km)	Positive strain polarity	20.15	11.50	9.83	1.78		28	1.0
	Negative strain poles	−10.1	−3.21	−3.08	−0.34			
Crossing the tunnel complex	Positive strain polarity	47.6	26.28	24.96	4.31		85.6	0.9
	Negative strain poles	−38.20	−24.25	−11.44	−1.57			
Through the gap between adjacent tunnel openings	Positive strain polarity	45.30	26.45	23.04	4.02	2.7		
	Negative strain poles	−37.52	−26.61	−11.65	−1.57			
Meeting in the tunnel (near the meeting surface)	Positive strain polarity	35.53	23.64	18.37	3.08	1.7	700	0.05
	Negative strain poles	−10.1	−6.12	−4.24	−0.50			
Meeting in the tunnel (near the tunnel wall)	Positive strain polarity	23.85	9.98	9.42	2.15	1.7	400	0.05
	Negative strain poles	−4.82	−3.12	−2.06	−0.24			

Source(s): Authors own work

It can be seen from Table 1 that under the tunnel aerodynamic effect, the high speed train window glass is subject to medium and low strain rates, of which the maximum strain rate (medium strain rate) occurs at the moment when the glass near the meeting face meets the nose of the opposite train in the tunnel; the maximum principal stress of the passenger compartment window glass of the high speed train resulting from the tunnel aerodynamic effect occurs at the corresponding time when the train passes through the tunnel groups, and does not exceed 5 MPa, which is lower than the design strength value of tempered glass (the design strength value of the middle part under conventional static pressure is 84 MPa). However, the influence of strain rate change and fatigue effect on glass strength shall be considered in the design of the bearing performance of high speed train window glass.

3.3 Bearing characteristics of high speed train window glass and tunnel aerodynamic load

The above measurement results show that the strain response of high speed train window glass surface induced by tunnel aerodynamic effect is a variation process of dynamic fatigue. The high speed train window glass is a typical composite structure of "hollow layer + laminated glass". The dynamic pressure acting on the glass surface will only affect the air transfer time of the hollow layer, and will not affect the load distribution ratio of the two pieces of glass. Based on the ideal gas law, if the temperature change of the gas in the hollow layer of the hollow glass is not considered, the following equation can be obtained.

$$P_0 V_0 = (P_0 + \Delta p)(V_0 - \Delta V) \tag{2}$$

where, P_0 is the initial gas pressure of the hollow layer of the hollow glass, typically 1 atm (1.013×10^5 Pa); V_0 is the initial volume of the hollow layer; ΔV is the volume change of the hollow layer after load bearing; Δp is the pressure change of the hollow layer.

Under the tunnel aerodynamic load p_0 (actually manifested as the pressure difference between the inside and outside of the car at the glass under test, regarded as uniform pressure), the two pieces of glass of the hollow glass will undergo synergistic deformation. Assuming that the deflections at the same position of the two pieces of glass are w_1 and w_2, respectively, and integrating the whole area of the hollow glass, the volume change of the hollow layer under the action of p0 can be obtained as (Liu, Bao, Qiu, Wan, & Wang, 2011)

$$\Delta V = \left| \oint (w_1 - w_2) \mathrm{d}\sigma \right| \tag{3}$$

Since the edges of the two pieces of hollow glass are supported by adhesive, the four sides can be regarded as simply supported. Based on the principle of load transmission by gas pressure change of the hollow layer, the deflections w_1 and w_2 of the two pieces of laminated glass of hollow glass can be calculated according to the following formula (Yuan, 1988):

$$w_1(x,y) = \frac{16p_1}{D_1\pi^6} \sum_{m=1}^{\infty} \sum_{n=1}^{\infty} \frac{\sin\frac{m\pi x}{a} \sin\frac{n\pi y}{b}}{mn\left(\frac{m^2}{a^2} + \frac{n^2}{b^2}\right)} \tag{4}$$

$$w_2(x,y) = \frac{16p_2}{D_2\pi^6} \sum_{m=1}^{\infty} \sum_{n=1}^{\infty} \frac{\sin\frac{m\pi x}{a} \sin\frac{n\pi y}{b}}{mn\left(\frac{m^2}{a^2} + \frac{n^2}{b^2}\right)} \tag{5}$$

where, x and y are the values of horizontal and vertical ordinates, respectively, m and n are series, taken as 1, 3, 5 . . .; a and b are the length of the long and short sides of the glass, respectively, D_1 and D_2 are the rigidity of the first piece of glass (facing the outside of the car) and the second piece of glass (facing the inside of the car), respectively, p_1 and p_2 are the air pressure difference between the two sides of the first and second pieces of glass, respectively, with values $p_1 = p_0 - \Delta p$, $p_2 = \Delta p$, respectively.

Substituting Equations (4) and (5) into Equation (3) and integrating them, and taking $m = 3$ and $n = 3$, a more accurate calculation formula can be obtained as follows

$$\Delta V = \frac{64a^5b^5}{\pi^8}\left(\frac{p_0 - \Delta p}{D_1} - \frac{\Delta p}{D_2}\right) \tag{6}$$

Since the two substrates of the hollow glass of the high speed train window glass are laminated glass, the rigidity calculation formula is as follows

$$D_1 = \frac{E{h_{1eq}}^3}{12(1-\mu^2)} \tag{7}$$

$$D_2 = \frac{E{h_{2eq}}^3}{12(1-\mu^2)} \tag{8}$$

where, D_1 and D_2 are the rigidity of the first and second pieces of laminated glass, respectively, h_{1eq} and h_{2eq} are the equivalent thickness of the first and second pieces of laminated glass, respectively.

With the interlaminar shear effect of the film and the contribution of the film thickness considered, and assuming that the thickness of the two substrates constituting the laminated glass is equal, the equivalent thickness h_{eq} of each piece of glass can be expressed as

$$h_{eq} = \sqrt{\frac{h_{e,df}^3}{h + 2\tau h_s}} \tag{9}$$

Where,

$$h_{e,df} = \sqrt[3]{2h^3 + 12\tau I_s}$$

$$I_s = \frac{h(h+h_v)^2}{2}$$

$$h_s = h + h_v$$

$$\tau = \frac{1}{1 + 9.6\frac{h_v E I_s}{G h_s^2 b^2}}$$

where, τ is the shear transfer coefficient of the PVB film of the laminated glass; $h_{e,df}$, I_s and h_s are coefficients related to the thickness of the laminated glass substrate and film; h and h_v are the thickness of the glass substrate and film in the laminated glass, respectively, G is the shear modulus of the PVB film.

The values of h_{1eq} and h_{2eq} can be obtained by substituting the thickness of the glass substrate and the film in the first and second pieces of laminated glass into Equation (9), respectively.

Since PVB film is a strain rate and temperature sensitive material, its shear modulus is related to temperature and the time of action on film, and affects the equivalent thickness and anti-deformation performance of laminated glass. The original data of the PVB film is measured according to the *Testing Method of Laminated Glass Interlayer Shear Modulus* (GB/T 32061-2015), and the relation between action time and shear modulus of PVB film at different temperature conditions is obtained, as shown in Figure 8.

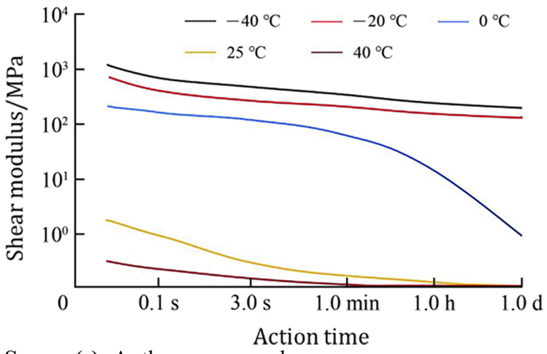

Source(s): Authors own work

Figure 8.
Relation curve between action time and shear modulus at different temperature conditions

It can be seen from Figure 8 that the shear modulus of PVB film obviously decreases with the increase of temperature and action time.

According to the test results given in Table 1, the action time of aerodynamic effects caused by the high speed train passing through different parts of the tunnel can be obtained. Combing with the relation curve in Figure 8, the appropriate shear modulus of PVB film can be selected and substituted into Equations (7) to (9) to obtain the equivalent thickness and rigidity of laminated glass under corresponding conditions. It can be seen from the calculation results that the dynamic equivalent thickness and rigidity of laminated glass decrease with the decrease of the shear modulus of PVB film. Therefore, the longer the load application time, the worse the dynamic bearing capacity of high speed train window glass. Based on the quantitative calculation with Equation (6), ΔV can be obtained and substituted into Equation (2), so that a quadratic equation with one unknown about Δp can be obtained, and then Δp can be accurately and quantitatively calculated.

Under the tunnel aerodynamic effect, the maximum tensile stress of the two pieces of laminated glass of the hollow glass of the high speed train is at its center, and the calculation formula (Yuan, 1988) is as follows

$$\sigma_{1\max} = f\frac{(p_0 - \Delta p)b^2}{{h_{1\mathrm{eq}}}^2} \tag{10}$$

$$\sigma_{2\max} = f\frac{\Delta p b^2}{{h_{2\mathrm{eq}}}^2} \tag{11}$$

Where, f is the coefficient related to the ratio of the length of the long and short sides of the glass; $\sigma_{1\max}$ and $\sigma_{2\max}$ are the maximum principal stresses of the first and second pieces of laminated glass of the hollow glass of the train, respectively.

According to the test results in Table 1, the tunnel aerodynamic load can be inverted. The aerodynamic load caused by the train entering the tunnel is taken as the calculation example. It can be obtained from the results of Figure 4 and Table 1 that the maximum principal stress peak of the glass under test resulting from the tunnel aerodynamic pressure is 2.65 MPa after the glass under test enters the tunnel entrance for about 3.7-3.8 s; the action time of corresponding maximum strain rate at this moment is 0.7 s; the corresponding ambient temperature when the strain is measured is 25℃, and the corresponding shear modulus is 0.8 MPa as shown in Figure 8. According to Equation (9), the equivalent thickness of the first and second pieces of laminated glass is calculated to be 8.69 and 7.31 mm, respectively. According to the length and width of the train window glass, f is 0.5688 (Yuan, 1988) as shown in the table. The above parameters are substituted into Equation (11), and Δp is calculated to be 389 Pa. Based on Equations (2) to (6), the corresponding maximum tunnel aerodynamic load p_0 acting on the glass under test is calculated to be 1,042.5 Pa.

With the above analysis method, the stress calculation and strength checking can also be carried out on the glass (windshield glass, cab side window glass, etc.) of other parts of the high speed train based on the overall pressure distribution relationship of the high speed train body according to the p_0 value obtained by inversion.

4. Conclusions

(1) When a high speed train passes through a tunnel, the window glass is subject to the alternating action of positive and negative aerodynamic loads, showing the typical fatigue load condition characterized by transient alternation of positive and negative strains, which is especially prominent when the train passes through a tunnel group.

(2) The maximum principal stress of the passenger compartment window glass of high speed train resulting from the tunnel aerodynamic load does not exceed 5 MPa and the design value of glass strength, and the maximum value occurs at the corresponding time when the train passes through the tunnel group. Under the tunnel aerodynamic effect, the high speed train window glass is subject to medium and low strain rates, and the maximum strain rate occurs at the moment when the glass near the meeting face met the nose of the opposite train in the tunnel.

(3) The shear modulus of the laminated glass PVB film is sensitive to temperature and action time. The dynamic equivalent thickness and rigidity of the laminated glass constituting the high speed train window glass decreases with the increase of the action time of the tunnel aerodynamic load, and its dynamic bearing capacity also gradually decreases with the increase of time.

(4) The action time of tunnel aerodynamic load and the influence of fatigue on glass strength shall be considered for the design of load-bearing performance of high speed train window glass.

References

Academy of Railway Sciences (2009). *Test report on the aerodynamic effect of the tunnel of Wu-guang passenger line*. China: Report of the Academy of Railway Sciences.

Academy of Railway Sciences, Chengdu Railway Bureau, Ministry of Railways (2005). *Comprehensive test Report on 200 km · h^{-1} speed Increase of sui-yu line*. China: Report of the Academy of Railway Sciences.

Chen, H., Zhang, Y., He, D., & Huang, C. (2014). Experimental study on the basic laws of the aerodynamic effect of 350 km · h^{-1} high speed railway tunnel. *China Railway Science*, *35*(1), 55–59.

Deng, G. X., Ma, W., Peng, Y., Wang, S., Yao, S., & Peng, S. (2021). Experimental study on laminated glass responses of high speed trains subject to windblown sand particles loading. *Construction and Building Materials*, *300*, 124332.

Doi, T., Ogawa, T., Masubuchi, T., & Kaku, J. (2010). Development of an experimental facility for measuring pressure waves generated by high speed trains. *Journal of Wind Engineering and Industrial Aerodynamics*, *98*(1), 55–61.

Iyer, R. S., Kim, D. H., & Kim, H. D. (2018). Prediction of entry compression waves induced by a high speed train entering tunnel. *Journal of Mechanical Science and Technology*, *32*(11), 5285–5292.

Jing, L., Liu, K., & Ren, M. (2019). The transient response of car body and side windows for high speed trains passing by each other in a tunnel. *Composites Part B: Engineering*, *166*, 284–297.

Ko, Y., Chen, C. H., Hoe, I. T., & Wang, S. T. (2012). Field measurements of aerodynamic pressures in tunnels induced by high speed trains. *Journal of Wind Engineering and Industrial Aerodynamics*, *100*(1), 19–29.

Liu, X., Bao, Y., Qiu, Y., Wan, D., & Wang, X. (2011). In-situ detection technology for failure of curtain-wall insulating glass. *China Civil Engineering Journal*, *44*(11), 52–58.

Nie, X., Chen, W. W., Sun, X., & Templeton, D. W. (2007). Dynamic failure of borosilicate glass under compression/shear loading experiments. *Journal of the American Ceramic Society*, *90*(8), 2556–2562.

Ozawa, S. (1979). *Studies on the micro-pressure wave radiated from a tunnel exit* (p. 1121). RTRI, Report No.

Peng, Y., Ma, W., Wang, S. M., Wang, K., & Gao, G. (2019). Investigation of the fracture behaviors of windshield laminated glass used in high speed trains. *Composite Structures*, *207*, 29–40.

Qian, C., Zheng, Z., Yu, J., & Li, S. (2013). Dynamic response of side windows of high speed trains subjected to crossing air pressure pulse. *Journal of Mechanical Engineering*, *49*(9), 30–36.

Real, T., Zamorano, C., Ribes, F., & Real, J. I. (2015). Train-induced vibration prediction in tunnels using 2D and 3D FEM models in time domain. *Tunnelling and Underground Space Technology*, *49*, 376–383.

Shi, D. (2002). The transient response analysis of side windows on high speed trains under the pressure wave of encountering another train. *Rolling Stock*, *40*(4), 17–19, 1.

Tian, H. (2015). Development of research on aerodynamics of high speed rails in China. *Strategic Study of CAE*, *17*(4), 30–41.

Tian, H., Yao, S., & Yao, S. (2000). Influence of the air pressure pulse on car-body and side-windows of two meeting trains. *China Railway Science*, *21*(4), 6–12.

Wang, G. (2020). *Study on cracking reasons and optimizing measures of side window glass of intercity EMU*. MA, thesis, Beijing: Beijing Jiaotong University.

Wang, L., Luo, J., Gao, L., Li, F., & Li, Z. (2020). The law of transient pressure in the process of 350 km/h high speed train entering a tunnel. *China Civil Engineering Journal*, *53*, 252–257, Supplement 1.

Woods, W. A., & Pope, C. (1979). On the range of validity of simplified one-dimensional theories for calculating unsteady flows in railway tunnels. *Proceedings of 3rd International Symposium on the Aerodynamics and Ventilation of Vehicle Tunnels, British Hydromechanics Research Association (BHRA)*, Sheffield (pp. 115–133), Paper D2.

Yuan, W. (1988). *Handbook of engineering mechanics*. Beijing: China Coal Industry Publishing House.

Zhao, Y., Ma, W., Cheng, A., & Zhang, Q. (2012). *Aerodynamic effect of high speed railway tunnel*. Beijing: China Railway Publishing House.

Corresponding author
Xiaogen Liu can be contacted at: lxg@ctc.ac.cn